Molecular Therapy
Nucleic Acids
Original Article

lncRNA Xist regulates sevoflurane-induced social and emotional impairment by modulating miR-98-5p/EDEM1 signaling axis in neonatal mice

Lili Xu,[1] Qi Xu,[1] Shaobing Dai,[1] Cuicui Jiao,[1] Yingying Tang,[1] Jiaqian Xie,[1] Hui Wu,[1] and Xinzhong Chen[1]

[1]Department of Anesthesiology, Women's Hospital, Zhejiang University School of Medicine, Hangzhou, Zhejiang Province, China

Long non-coding RNA (lncRNA) X-inactive specific transcript (Xist) is involved in apoptosis and inflammatory injury. This study aimed to assess the role of lncRNA Xist in sevoflurane-induced social and emotional impairment and neuronal apoptosis in neonatal mice and hippocampal neuronal cells. The performance in social and emotional tests and the expression levels of lncRNA Xist and microRNA (miR)-98-5p after sevoflurane exposure were measured. Moreover, the effects of suppression of lncRNA Xist on neuronal apoptosis and endoplasmic reticulum (ER) stress were determined. Subsequently, the association among lncRNA Xist, miR-98-5p, and ER degradation-enhancing α-mannosidase-like 1 protein (EDEM1) was explored. Our results showed that lncRNA Xist increased, miR-98-5p decreased, and social and emotional impairment appeared after sevoflurane exposure. Furthermore, suppression of lncRNA Xist improved sevoflurane-induced social and emotional impairment and reduced sevoflurane-induced neuronal apoptosis and ER stress *in vivo* and *in vitro*. Moreover, lncRNA Xist negatively regulated miR-98-5p expression, and it contributed to sevoflurane-induced neuronal apoptosis and ER stress by sponging miR-98-5p. Additionally, EDEM1 was identified as a target of miR-98-5p. Our findings revealed that the knockdown of lncRNA Xist ameliorates sevoflurane-induced social and emotional impairment through inhibiting neuronal apoptosis and ER stress by targeting the miR-98-5p/EDEM1 axis.

INTRODUCTION

Mounting evidence demonstrates that early long/repeated exposures to sevoflurane can cause neurobehavioral disorders, including spatial, non-spatial, and fear-conditioning learning deficits; anxiety-related behaviors; and motor reflex deficits. Moreover, it can impact the socio-emotional development in rodents and nonhuman primates.[1,2] Recently, the possible underlying molecular and cellular mechanisms have been unveiled; these include neuronal apoptosis, neurogenesis alterations, disruption of axon guidance, increase or decrease in dendrite outgrowth, alteration of synaptic functions, and aberrant synaptogenesis and neural circuit formation.[3,4] However, the precise mechanisms underlying these alterations have not been fully elucidated.

A recent report has shown that long non-coding RNAs (lncRNAs) have important effects on some neurological diseases, such as spinal cord injury (SCI).[5] lncRNA X-inactive specific transcript (Xist) has been postulated to be a cancer-related gene involved in the pathogenesis of SCI.[6] This study found that silencing lncRNA Xist contributed to ameliorating apoptosis and inflammatory injury in SCI models *in vivo* and *in vitro* through regulating microRNA (miR)-27a/Smurf1 signaling. Moreover, Gu et al.[5] suggested that the inhibition of lncRNA Xist could prevent neuronal apoptosis following SCI in mice, indicating that lncRNA Xist could be a promising molecular target for SCI therapy. miR-98-5p is a regulator of oxidative stress, apoptosis, and cell survival in numerous biological processes and cell types. Sun et al.[7] demonstrated that miR-98-5p decreases oxygen-glucose deprivation/reoxygenation (OGD/R)-induced neuronal injury through the activation of the Nrf2/ARE axis *in vitro*, highlighting that miR-98-5p has potential effects on cerebral ischemia/reperfusion injury and could become a new therapeutic target for neuroprotection.

Sevoflurane-mediated endoplasmic reticulum (ER) stress produces different effects on the distinct areas of the developmental hippocampus. Furthermore, inhibition of ER stress provides a potential preventive and therapeutic target for sevoflurane-induced long-term learning and memory deficits.[8] Related to ER stress, ER degradation-enhancing α-mannosidase-like 1 protein (EDEM1) is involved in the routing of misfolded glycoproteins for degradation in the cytoplasm and leaves the ER via non-COPII vesicles becoming degraded by basal autophagy.[9] Interestingly, Lin et al.[10] showed that naringenin alleviates hepatic apoptosis and ER stress and decreases DNA damage genes (C/EBP-homologous protein [CHOP], gadd45αa, and EDEM1) in larvae. Moreover, EDEM1 has been proven to play critical roles in protein misfolding, and it could become the future research focus and therapeutic target for Parkinson's disease (PD).[11]

Received 30 July 2020; accepted 9 April 2021;
https://doi.org/10.1016/j.omtn.2021.04.010.

Correspondence: Xinzhong Chen, Department of Anesthesiology, Women's Hospital, Zhejiang University School of Medicine, Hangzhou, Zhejiang Province, China.
E-mail: chenxinz@zju.edu.cn

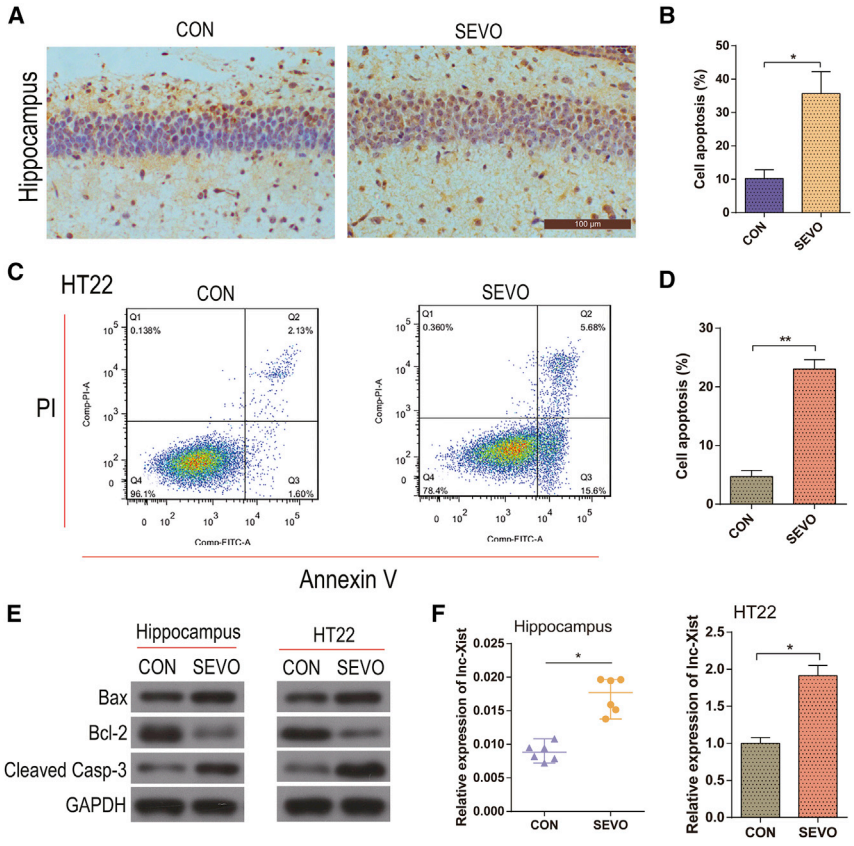

Figure 1. Sevoflurane (SEVO)-induced neuronal apoptosis in neonatal mice and HT22 cells

Neonatal mice were divided into two groups of six mice each. The SEVO group was exposed to 3.4% SEVO for 5 h, and the control group was exposed to air for 5 h. (A and B) TUNEL staining in the hippocampus of a mouse; representative images (A) and quantification (B). (C and D) Annexin V-FITC/PI staining and flow cytometry analysis; representative images (C) and quantification (D). (E) Representative images of western blot for Bax, Bcl-2, and cleaved caspase-3 in the hippocampus of a mouse and in cultured neurons. (F) Quantitative real-time PCR for lncRNA Xist in the hippocampus of a mouse and in cultured neurons. *$p < 0.05$, **$p < 0.01$. N = 6.

The role of lncRNA Xist in sevoflurane-induced neurotoxicity and the association of lncRNA Xist with miR-98-5p and EDEM1 in hippocampal neurons remain largely unknown. In the present study, we aimed to examine the role and the molecular mechanism of lncRNA Xist in sevoflurane-induced social and emotional impairment and neuronal apoptosis in neonatal mice.

RESULTS

Sevoflurane does not alter arterial blood pressure and arterial blood gas levels

After exposing the mice to 3.4% sevoflurane in air or to only air (to control mice) for 5 h, there were no signs of cardiorespiratory dysfunction. There were no significant differences in arterial oxygen pressure (PaO_2), blood oxygen saturation (SaO_2), power of hydrogen (PH), carbon dioxide partial pressure ($PaCO_2$), and mean arterial pressure (MAP) between the groups (Table S1). The data indicate that sevoflurane treatment has no harmful effects on the physiological parameters of the mice.

Sevoflurane increases lncRNA Xist and apoptosis in neonatal mice and HT22 cells

To investigate whether sevoflurane induced apoptosis, TUNEL staining was performed in the hippocampus of the mice after sevoflurane exposure. Increases in TUNEL-positive neurons could be observed both in representative images (Figure 1A) and by quantification (Figure 1B). To confirm sevoflurane-induced apoptosis in neurons, Annexin V-fluorescein isothiocyanate (FITC)/propidium iodide (PI) staining and flow cytometry analysis were performed. The results showed significant increases in the rate of apoptosis, including early and late apoptosis, after sevoflurane exposure (Figures 1C and 1D). Additionally, the levels of cleaved caspase-3, Bax, and Bcl-2 (markers for apoptosis) were assessed by western blot in hippocampal cells, showing increases in cleaved caspase-3 and Bax levels and decreases in Bcl-2 levels after sevoflurane exposure (Figure 1E). Finally, the expression of lncRNA Xist was determined by quantitative real-time polymerase chain reaction (PCR), showing that lncRNA Xist significantly increased after sevoflurane exposure (Figure S1). Our evidence indicates that sevoflurane treatment induces neuronal apoptosis and upregulates lncRNA Xist in the neurons of neonatal mice, which may contribute to sevoflurane-induced neurotoxicity.

Silencing lncRNA Xist attenuates sevoflurane-induced apoptosis in neonatal mice and HT22 cells

To ensure an effect of Xist small interfering (si)RNA on lncRNA Xist, the expression of lncRNA Xist was determined in neurons by quantitative real-time PCR, showing that lncRNA Xist expression significantly decreased after exposure to Xist siRNA (Figure 2A). To fully assess the role of lncRNA Xist on sevoflurane-induced neurotoxicity, we explored whether inhibition of lncRNA Xist downregulates the apoptosis caused by sevoflurane in neurons. Annexin V-FITC/PI staining and flow cytometry analysis revealed significant decreases in the rate of apoptosis, including early and late apoptosis, after co-exposure to sevoflurane and Xist siRNA (Figures 2B and 2C).

To evaluate the effects of lncRNA Xist on sevoflurane-induced neurotoxicity, small hairpin (sh)RNA Xist or shRNA negative control (NC; Ruibo Biotechnology, Guangzhou, China) was intracranially injected into the bilateral hippocampi of the mice (each side, 5 nmol every 2 days, a total of 4 injections). 1 day after the final injection, the mice

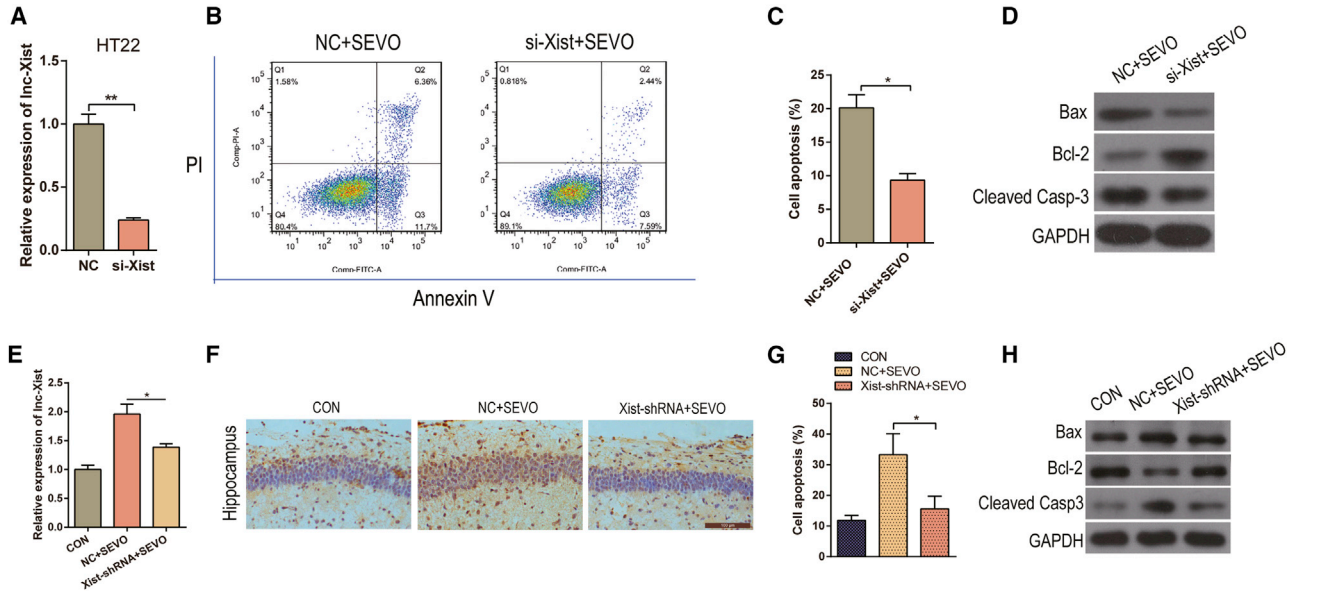

Figure 2. lncRNA Xist knockdown decreases SEVO-induced apoptosis in neonatal mice and in HT22 cells

Neonatal mice and cultured neurons were divided into two groups with six each. The SEVO group was exposed to 3.4% SEVO, and the control group was exposed to air for 5 h. The neonatal mice received stereotaxic intracranial injections with shRNA Xist or shRNA NC in the bilateral hippocampi (n = 6 in each group). 1 day after injection, SEVO treatment was conducted on these mice. (A) Quantitative real-time PCR for lncRNA Xist in neurons. (B and C) Annexin V-FITC/PI staining and flow cytometry analysis; representative images (B) and quantification (C). (E) Quantitative real-time PCR for lncRNA Xist to verify the efficiency of shRNA Xist in the hippocampus of a mouse. (F and G) TUNEL staining in the hippocampus of a mouse; representative images (E) and quantification (F). (D and H) Representative images of western blot for Bax, Bcl-2, and cleaved caspase-3 in neurons and in the hippocampus of a mouse. *$p < 0.05$, **$p < 0.01$. N = 6.

were exposed to sevoflurane. TUNEL staining revealed decreases in TUNEL-positive neurons in the hippocampi of mice after co-exposure to sevoflurane and shRNA Xist, as seen in representative images (Figure 2F) and by quantification (Figure 2G). Moreover, the exposure to sevoflurane significantly upregulated the expression of Bax and cleaved caspase-3, whereas significantly downregulating the expression of Bcl-2. Importantly, the expression of all of these proteins was decreased compared to the control group after co-exposure to Xist siRNA and sevoflurane in neurons (Figure 2D) and after co-exposure to shRNA Xist and sevoflurane in the hippocampus of the mice (Figure 2G). Our findings reveal that the silencing of lncRNA Xist reduces the apoptosis induced by sevoflurane in neonatal mice and in HT22 cells.

Suppression of lncRNA Xist expression attenuates sevoflurane-induced social and emotional impairment in neonatal mice

To evaluate the effects of lncRNA Xist on social and emotional behaviors of mice after sevoflurane exposure, the mice were subjected to the elevated plus maze, the open field test, and the social behavioral test after sevoflurane exposure. The elevated plus maze showed that, after sevoflurane exposure, neonatal mice that had received shRNA Xist displayed more entries into open arms and less time spent in the open arms compared to the shRNA NC group, whereas there was no difference in total distance traveled between the two groups (Figures 3A and 3B). The open field test results revealed that, after sevoflurane exposure, neonatal mice that had received shRNA Xist spent more time in the center of the open field and traveled longer total distances during the 5 min of open field exploration compared to the shRNA NC group (Figures 3C–3E). Moreover, shRNA Xist improved sevoflurane-induced social interaction impairments in neonatal mice as shown by the three-chamber social interaction test. We performed two social behavioral tests—the social preference and the social novelty tests—using the three-chamber sociability paradigm (Figure 3F). Neonatal sevoflurane-exposed mice had a deficiency in social interaction behaviors. Regarding social preference, mice that had received shRNA Xist spent markedly more time in the chamber with the novel mouse and interacting with the novel mouse compared to the shRNA NC group, whereas there was no difference in the time spent in the center chamber and in the chamber containing the novel object and interacting with the novel object between the two groups (Figures 3G and 3H). Regarding social novelty, mice that had received shRNA Xist spent markedly more time in the chamber with the second novel mouse and interacting with the second novel mouse compared to the shRNA NC group, whereas there was no difference in the time spent in the center chamber and in the chamber containing the novel mouse and interacting with the novel mouse between the two groups (Figures 3I and 3J). Our findings confirm that social and emotional performances are impaired in neonatal mice exposed to sevoflurane, and this can be reverted by lncRNA Xist suppression.

miR-98-5p is a target of lncRNA Xist in HT22 cells

To explore the downstream modulatory mechanism of lncRNA Xist, possible targets of lncRNA Xist were assessed by Starbase software.

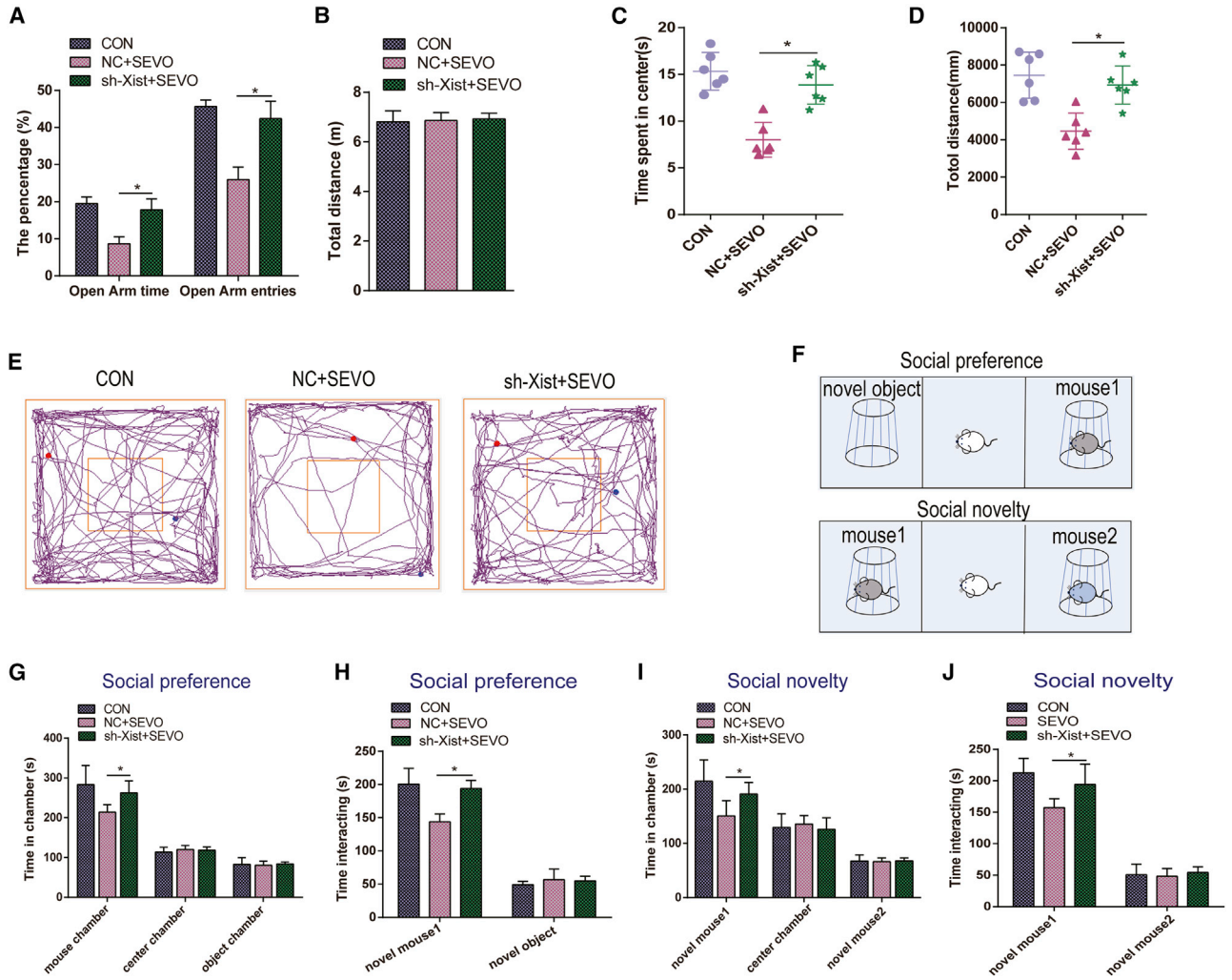

Figure 3. lncRNA Xist knockdown reverses SEVO-induced social and emotional impairment in neonatal mice

(A and B) Elevated plus maze 8 weeks after SEVO exposure. (A) Percentage of entries into open arms and percentage of time spent in the open arms. (B) Total distance run during the trial (locomotion index). (C–E) Open field test 8 weeks after SEVO exposure. (C) Time spent in the center of the open field during 5 min of open field exploration. (D) Total distance run during 5 min of open field exploration. (E) Movement tracks showing 5 min of open field exploration. (F) Three-chamber test 8 weeks after SEVO exposure. Three-chamber sociability paradigm. (G) Time spent in the center chamber, the chamber containing the novel mouse (novel mouse 1), or the novel object. (H) Time spent interacting with the novel mouse (novel mouse 1) or the novel object. (I) Time spent in the center chamber, the chamber containing the novel mouse, or the chamber containing the second novel mouse (novel mouse 2). (J) Time spent interacting with the novel mouse or the second novel mouse (novel mouse 2). *$p < 0.05$, **$p < 0.01$. $N = 6$.

We found that miR-98-5p is a target of lncRNA Xist in HT22 cells (Figures 4A and 4B). A quantitative real-time PCR was performed to confirm changes in miR-98-5p levels in these cells. The levels of miR-98-5p were significantly altered after modification of lncRNA Xist levels (Figure 4C). To further verify the interaction between lncRNA Xist and miR-98-5p, a dual-luciferase reporter assay was performed. The luciferase activity of lncRNA Xist wild type (WT) was markedly suppressed in miR-98-5p-overexpressing cells, but no obvious change in the luciferase activity of lncRNA Xist mutant (Mut) was observed (Figure 4D). Anti-AGO2 RNA immunoprecipitation (RIP) was also performed in HT22 cells. A quantitative real-time PCR confirmed that the levels of both lncRNA Xist and miR-98-5p significantly increased, indicating that lncRNA Xist, miR-98-5p, and AGO2 formed a complex in miR-98-5p-transfected HT22 cells (Figure 4E). Together, these data suggest that lncRNA Xist targets miR-98-5p to inhibit its translation in HT22 cells.

Overexpression of miR-98 decreases sevoflurane-induced apoptosis through CHOP and Tribbles-related protein 3 (Trib3) ER stress signaling pathways

Our previous results indicated that sevoflurane exposure downregulated miR-98-5p in neonatal mice and HT22 cells (Figures 5A and 5B). To further determine whether lncRNA Xist regulated apoptosis in HT22 cells after sevoflurane exposure by targeting miR-98, miR-98

was overexpressed by transfection of miR-98 mimic in HT22 cells. Annexin V-FITC/PI staining and flow cytometry analysis indicated a significant decrease in the rate of apoptosis, including early and late apoptosis, after co-exposure to sevoflurane and miR-98 mimic (Figures 5D and 5E). We also observed that sevoflurane significantly enhanced the expression of cleaved caspase-3 and Bax, whereas significantly downregulating the expression of Bcl-2. The expression of these proteins was the opposite to the control group after co-exposure to sevoflurane and miR-98 mimic (Figure 5F).

Furthermore, CHOP, a vital part of the ER stress reactive machinery, favors ER stress-induced apoptosis via inhibition of autophagy *in vitro*. TRIB3 is a critical factor in various cellular processes; upregulation of TRIB3 triggers apoptosis and thereby promotes the suppression of cell growth. To additionally determine whether sevoflurane caused ER stress, a western blot analysis was performed in the hippocampus of the mice and in neurons, revealing increases in CHOP and Trib3 levels after sevoflurane exposure, as seen in representative images (Figures 5G and 5H). Accordingly, we concluded that miR-98 overexpression decreased the apoptosis induced by sevoflurane in HT22 cells. The silencing of lncRNA Xist significantly decreased the expression of the ER stress markers CHOP and Trib3 and the cell apoptosis markers cleaved caspase-3 and Bax and significantly upregulated the expression of Bcl-2, whereas inhibiting lncRNA Xist concurrently to suppressing miR-98 inversed these protein expression levels in neurons (Figures 5I and 5J). We confirmed that lncRNA Xist regulates apoptosis in neural cells by sponging miR-98-5p and that lncRNA Xist might play a key role in sevoflurane-induced neurotoxicity via regulating miR-98.

miR-98-5p targets EDEM1 by suppressing translation in HT22 cells

To explore the downstream modulatory mechanism of miR-98-5p, the possible targets of miR-98-5p were assessed by TargetScan software. We found that EDEM1 was a potential target of miR-98-5p (Figures 6A and 6B). To further verify the interaction between miR-98 and EDEM1, a dual-luciferase reporter assay was performed. We found that the luciferase activity of EDEM1 WT was markedly suppressed in miR-98-overexpressing cells, but no obvious change in the luciferase activity of EDEM1 Mut was observed (Figure 6C). Additionally, a quantitative real-time PCR was performed to determine EDEM1 expression in HT22 cells after transfection with NC mimic or miR-98 mimic. The overexpression of miR-98 significantly inhibited EDEM1 expression, whereas the suppression of miR-98 markedly increased EDEM1 expression (Figure 6D). Furthermore, the western blot analysis indicated that the protein expression of EDEM1 displayed consistent changes in HT22 cells after transfection with miR-98 mimic and NC mimic (Figure 6E). The above facts show that EDEM1 is a potential target of miR-98 and is negatively modulated by miR-98.

Sevoflurane increases EDEM1 expression in neonatal mice and HT22 cells, and miR-98 is involved in apoptosis through regulating EDEM1 in HT22 cells

As a mannosidase-like protein, EDEM1 conscripts misfolded glycoproteins from the calnexin/calreticulin-folding circulation to downstream ER-associated degradation signaling. We assessed the interaction among lncRNA Xist, miR-98-5p, and EDEM1 and observed that the silencing of lncRNA Xist significantly decreased EDEM1 expression, whereas the inhibition of lncRNA Xist concurrently with the suppression of miR-98 inversed EDEM1 expression levels in neurons (Figure S2). To explore the role of EDEM1 in sevoflurane-induced neuronal apoptosis, the expression of EDEM1 was determined in mouse brain and in neurons by quantitative real-time PCR and western blot analysis, showing that EDEM1 expression significantly increased after sevoflurane exposure (Figures 6G–6J). Immunofluorescence staining results also showed that EDEM1 expression increased in neurons after sevoflurane exposure, as seen in representative images and by quantification (Figure 6K). These results suggest that sevoflurane upregulates EDEM1 expression and induces ER stress in neonatal mice and in neurons. The effects of the simultaneous suppression of Xist and overexpression of EDEM1 on ER stress in neurons were explored. The results showed that the effects of Xist inhibition alone on the ER stress markers CHOP and Trib3 and the cell apoptosis markers cleaved caspase-3, Bax, and Bcl-2 in neurons were reversed after the suppression of Xist concurrently to the overexpression of EDEM1 (Figures 6L and 6M). Collectively, our evidence indicated that sevoflurane treatment upregulates EDEM1 expression and induces ER stress in neonatal mice and in neurons, which may contribute to sevoflurane-induced neuronal apoptosis. We also confirmed that lncRNA Xist regulates ER stress in neural cells through modulating EDEM1 and that lncRNA Xist might play a key role in sevoflurane-induced neurotoxicity via regulating EDEM1 (Figures 6N and 6O).

DISCUSSION

In the present study, the effects and mechanisms of lncRNA Xist on sevoflurane-induced neurotoxicity were investigated using neonatal mice and hippocampal cells. Our results showed that sevoflurane exposure led to poor performance of neonatal mice in the elevated plus maze, the open field test, and the three-chamber social interaction test and that it increased lncRNA Xist and EDEM1 expression in hippocampal neurons. Silencing of lncRNA Xist significantly improved the performance of the mice in these social and emotional behavioral tests and reduced sevoflurane-induced apoptosis and ER stress *in vitro* and *in vivo*. Further *in vitro* studies showed that lncRNA Xist negatively regulated miR-98-5p expression and that lncRNA Xist regulated sevoflurane-induced apoptosis and ER stress in hippocampal neurons by sponging miR-98-5p. These findings suggest a key role of lncRNA Xist in sevoflurane-induced neurotoxicity.

Anesthesia can induce neurotoxicity and neurocognitive impairments in young mice.[12,13] Previous data have shown that exposure to sevoflurane induces both learning deficits and abnormal social behaviors resembling autism spectrum disorders in neonatal mice.[14,15] Recent studies concluded that early exposure to anesthesia could have lasting effects on emotional and social development, and rodent behavioral models were an excellent instrument to investigate long-term socio-emotional general anesthesia-caused disorders in humans.[16,17] In our investigation, we further confirmed that exposure

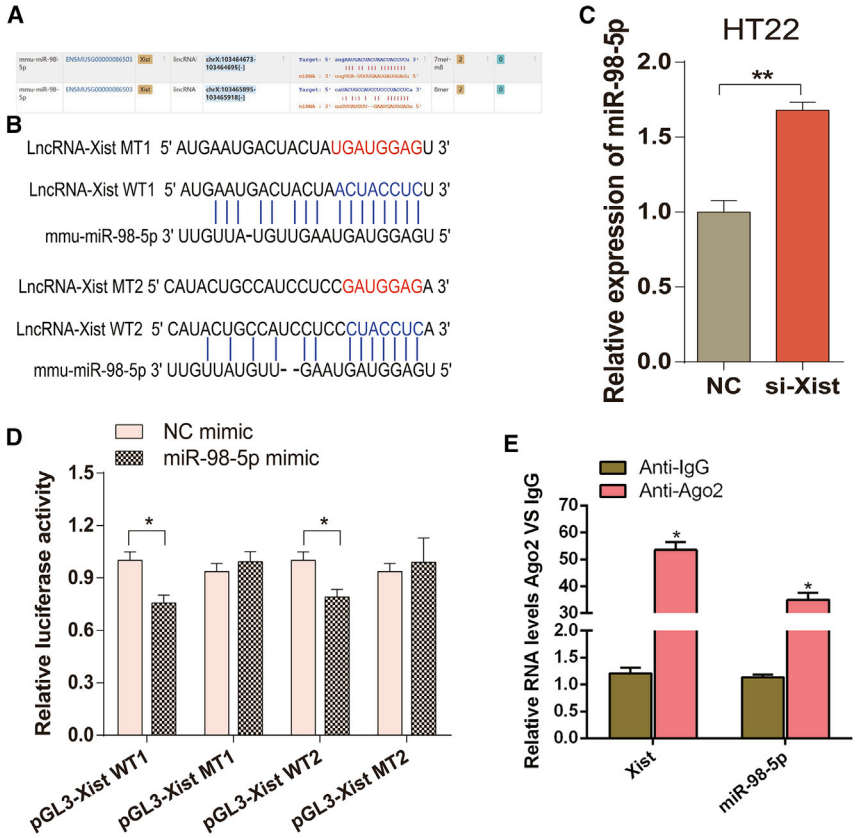

Figure 4. Binding between lncRNA Xist and miR-98-5p

(A) lncRNA Xist predicted to bind miR-98-5p by Starbase software. (B) Bioinformatics analysis predicts binding of miR-98-5p to the 3′ UTR of lncRNA Xist in mice. (C) Knockdown of lncRNA Xist by siRNA in HT22 neurons. Transfection with NC mimic used as control. Quantitative real-time PCR for miR-98-5p levels. (D) Wild-type mRNA (3′ UTR) and mRNA with a mutation in the 3′ UTR miR-98-5p-binding site (3′ UTR Mut) of lncRNA Xist. A dual-luciferase reporter assay conducted by miR-98-5p-modifying plasmids and 3′ UTR plasmids of lncRNA Xist. (E) Quantitative real-time PCR for RNA levels of lncRNA Xist and miR-98-5p in miR-98-5p-transfected neurons using anti-AGO2 RIP. *$p < 0.05$, **$p < 0.01$.

to sevoflurane causes deficits in social and emotional behavior in neonatal mice, as shown by the altered results in the elevated plus maze, the open field test, and the three-chamber social interaction test. Collectively, these findings indicate that exposure to sevoflurane impairs social and emotional behaviors in neonatal mice and that this may have lasting influences on emotional and social development.

An increasing number of studies have evidenced the critical role of lncRNAs in the pathogenesis of numerous neurological processes. In particular, lncXist is considered one of the most enhanced lncRNAs and is associated with apoptosis. Yue et al.[18] demonstrated that the expression of lncRNA Xist was enhanced *in vivo* and *in vitro* in Alzheimer's disease (AD) models. Suppression of lncRNA Xist positively modulated BACE1 and negatively modulated miR-124 expression in N2a cells. lncRNA Xist could be a new potential focus for the treatment of AD. Moreover, Gu et al.[5] confirmed that inhibition of lncRNA Xist suppresses neuronal apoptosis in a mice model of SCI and that the protective effects of lncRNA Xist inhibition might be regulated by the phosphorylation of AKT and miR-494. Our results showed that the expression of lncRNA Xist is increased *in vivo* and *in vitro* after sevoflurane exposure and that the suppression of lncRNA Xist decreases sevoflurane-induced apoptosis and ER stress. We, thus, speculate that lncRNA Xist contributes to the development of sevoflurane-induced neurotoxicity via regulating apoptosis and ER stress.

Growing evidence from animal model studies has confirmed that as a stress-related microRNA (miRNA), miR-98-5p plays a key role in modulating oxidative stress, apoptosis, and cell survival in numerous biological processes and cell types. Sun et al.[7] demonstrated that miR-98-5p attenuates OGD/R-induced neuronal injury by the activation of the Nrf2/ARE pathway *in vitro*, indicating that miR-98-5p could be a target for cerebral ischemia/reperfusion injury treatment and a therapeutic target for neuroprotection. In this study, our bioinformatics analysis predicted miR-98-5p to be a molecular target of lncRNA Xist, which was verified by dual-luciferase reporter assay and anti-AGO2 RIP. We found that the overexpression of miR-98 decreased the apoptosis induced by sevoflurane in HT22 neurons. That is, the inhibition of lncRNA Xist significantly downregulated the cell apoptosis markers cleaved caspase-3 and Bax in HT22 cells, whereas this was reversed after inhibition of lncRNA Xist concurrently with miR-98. Based on our results, we speculate that lncRNA Xist negatively regulates miR-98-5p expression and that lncRNA Xist exerts its effects on apoptosis by sponging miR-98-5p in HT22 neurons.

As a protein quality control factor, EDEM1 was first known for its capacity to discern N-linked glycans in misfolded proteins by its mannosidase-like domain. Yang et al.[19] indicated that paraquat-enhanced EDEM, glucose-regulated protein 78, ER stress biomarker proteins, and CHOP activate the IRE1/ASK1/JNK cascade associated with apoptosis in SY5Y cells. Lin et al.[11] highlighted the key roles of the genes EDEM1, ATF4, and TRAF2 in the protein-misfolding process of PD, which makes them potential therapeutic targets for PD. In this study, our bioinformatics analysis predicted EDEM1 to be a molecular target of miR-98-5p, which was verified by the dual-luciferase reporter assay. Additionally, we found that sevoflurane exposure increased the expression of EDEM1 and of the ER stress markers CHOP and Trib3 in neonatal mice and in HT22 neurons. The silencing of lncRNA Xist decreased CHOP and Trib3 expression after

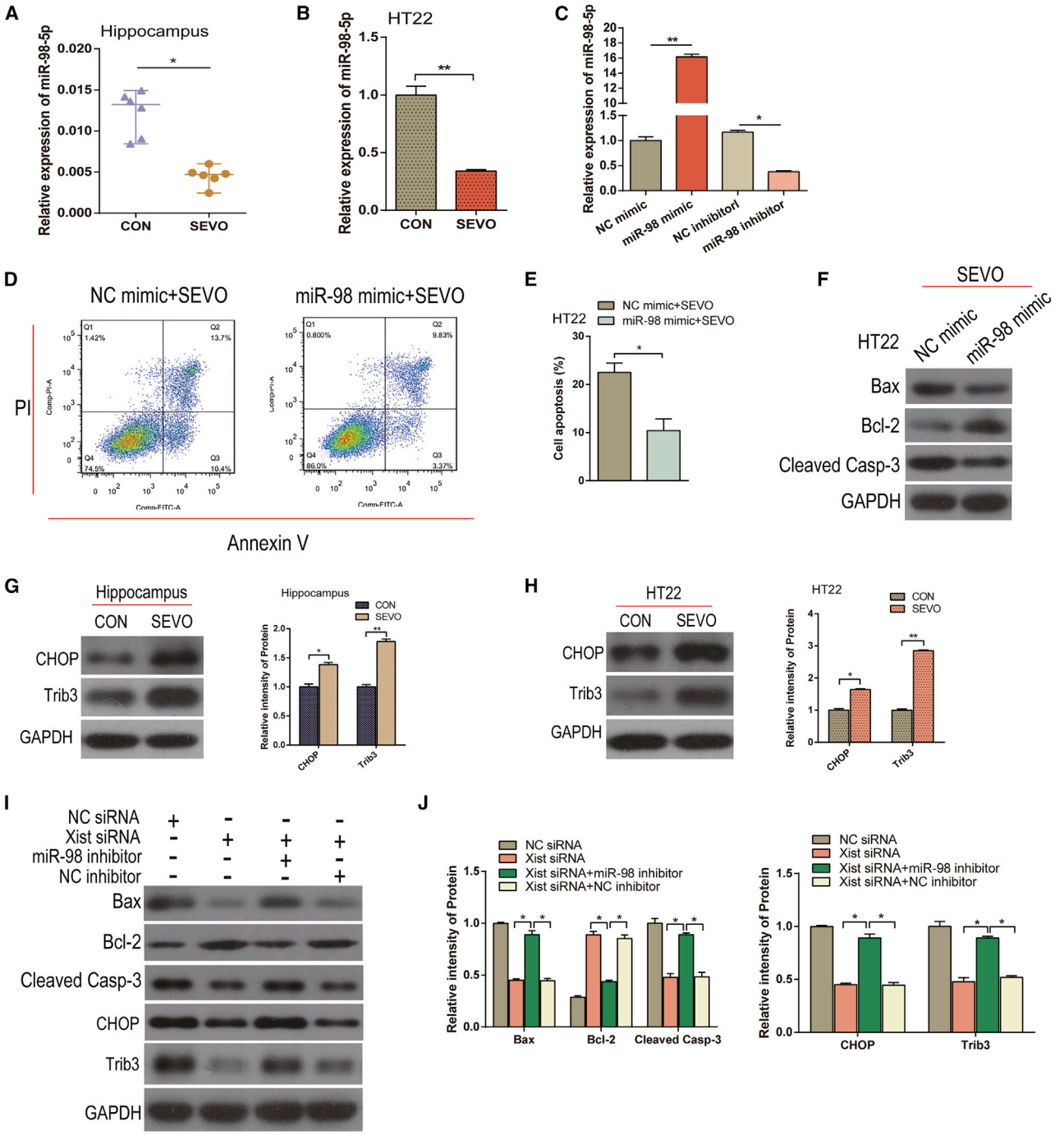

Figure 5. Effects of lncRNA Xist and miR-98-5p on SEVO-induced ER stress and apoptosis in HT22 cells

(A and B) Quantitative real-time PCR for miR-98-5p in the hippocampus of a mouse (A) and in neurons (B). (C) Quantitative real-time PCR for miR-98-5p to verify the efficiency of miR-98 mimic and miR-98 inhibitor in neurons. (D and E) Annexin V-FITC/PI staining and flow cytometry analysis; representative images (D) and quantification (E). (F–J) Western blot for Bax, Bcl-2, cleaved caspase-3, CHOP, and Trib3 in neurons and in the hippocampus of a mouse; representative images (F–I) and quantification (J). *$p < 0.05$, **$p < 0.01$.

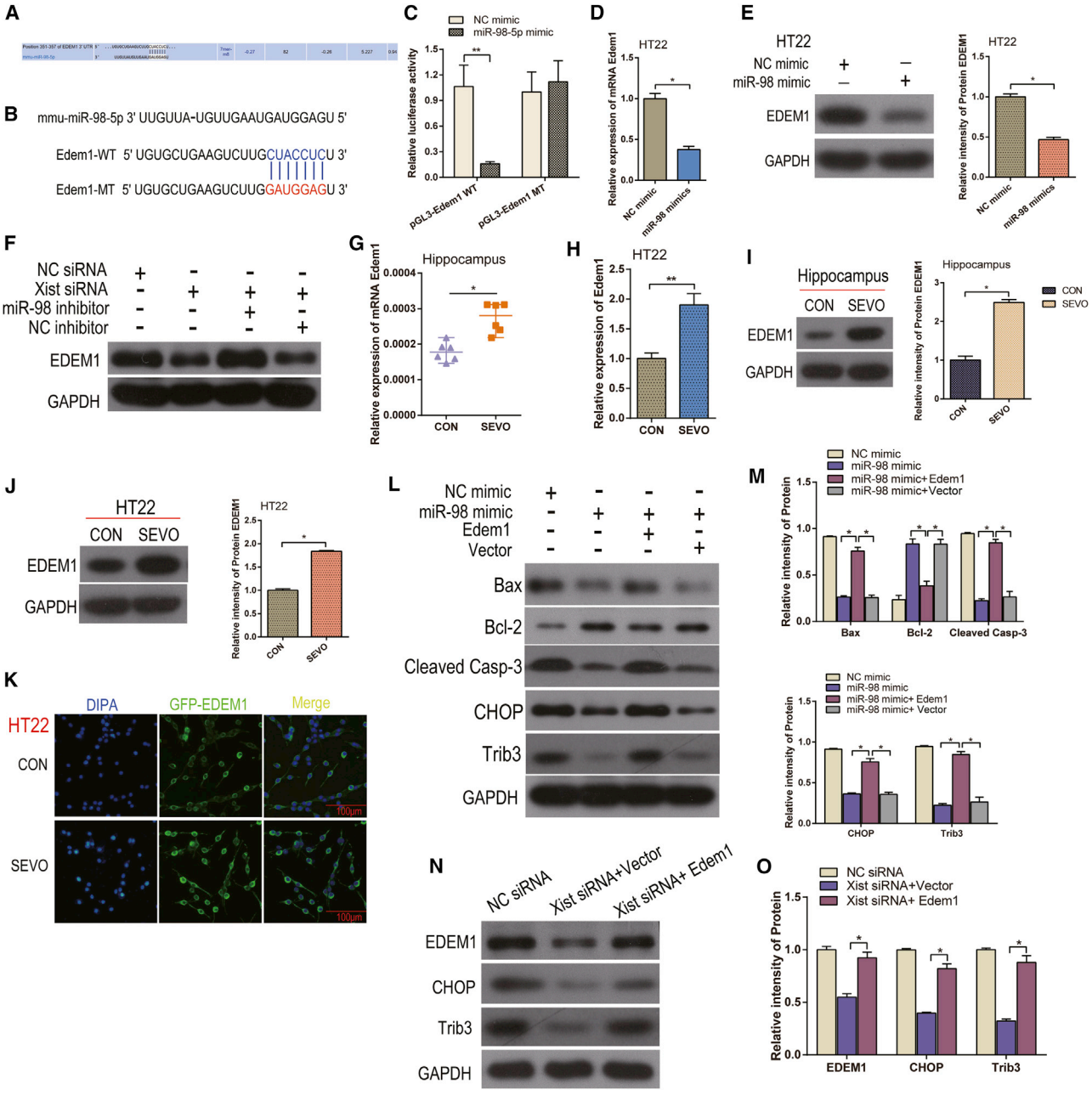

Figure 6. Binding between miR-98-5p and EDEM1 and its effects on SEVO-induced ER stress and apoptosis in HT22 cells

(A and B) Bioinformatics analysis predicts binding of miR-98-5p to the 3′ UTR of EDEM1 in mice. (C) Wild-type mRNA (3′ UTR) and mRNA with a mutation in the 3′ UTR miR-98-5p-binding site (3′ UTR Mut) of EDEM1. A dual-luciferase reporter assay conducted by miR-98-5p-modifying plasmids and 3′ UTR plasmids of EDEM1. (D) miR-98-5p overexpressed by miR-98-5p mimic in HT22 cells. Transfection with NC mimic used as control. Quantitative real-time PCR for EDEM1 levels. (E) Western blot for EDEM1 levels in miR-98-modified HT22 cells; representative images and quantification. (F) Western blot for EDEM1 levels in HT22 cells; representative images and quantification. (G and H) Quantitative real-time PCR for miR-98-5p in the hippocampus of a mouse and in neurons. (I and J) Western blot for EDEM1 in the hippocampus of a mouse and in neurons; representative images and quantification. (K) Immunofluorescence staining of EDEM1 in neurons; representative images and quantification. (L and M) Western blot for Bax, Bcl-2, cleaved caspase-3, CHOP, and Trib3 in neurons; representative images (L) and quantification (M). (N and O) Western blot for EDEM1, CHOP, and Trib3 in neurons; representative images (N) and quantification (O). *$p < 0.05$, **$p < 0.01$. N = 6.

sevoflurane exposure, which could be reversed by the inhibition of lncRNA Xist simultaneously to the overexpression of EDEM1. Collectively, these data confirm that EDEM1 is a downstream regulatory mechanism of lncRNA Xist/miR-98-5p, which regulates apoptosis and ER stress after exposure to sevoflurane, and that the effects of lncRNA Xist on apoptosis and ER stress in HT22 neurons are executed through the miR-98-5p/EDEM1 pathway. We also investigated the interaction among lncRNA Xist, miR-98-5p, and EDEM1 and found that the silencing of lncRNA Xist significantly decreased EDEM1 expression, whereas the inhibition of lncRNA Xist concurrently with the suppression of miR-98 inversed EDEM1 expression levels in neurons. These provide further evidence on the capacity of lncRNA Xist to sponge miR-98-5p as a competitive endogenous RNA (ceRNA); lncRNA Xist is predicted to act as a ceRNA to modulate EDEM1 by competitively binding to miR-98-5p.

In conclusion, these findings have revealed that downregulation of lncRNA Xist may contribute to mitigate sevoflurane-induced neurotoxicity in hippocampal neurons and social and emotional behavioral deficits in neonatal mice via inhibiting apoptosis and ER stress. The miR-98-5p/EDEM1 axis may be the downstream mechanism for the role of lncRNA Xist in the development of sevoflurane-induced neurotoxicity. Our results provide new evidence for the clinical concerns regarding sevoflurane anesthesia and could represent a promising strategy to prevent sevoflurane-induced neurotoxicity. Further studies are still required to verify our findings.

MATERIALS AND METHODS

Ethics statement

The study protocol was approved by the Zhejiang University Institutional Review Board of Animal Studies (ZJU2019-16778). All experimental procedures were performed in accordance with The Ministry of Science and Technology of the People's Republic of China's *Guidance Suggestions for the Care and Use of Laboratory Animals*.[20]

Animals and anesthesia treatment

Male C57BL/6 mice of 6 days of age (2.9−3.8 g) were purchased from the Laboratory Animal Center of Zhejiang University (2019000624485). Each experimental condition group had a balanced number of littermate controls. All animals were housed in standard animal cages under conventional housing conditions (12 h light-dark cycle and 22 ± 1°C). The mice were randomly allocated to the sevoflurane group (exposed to 3.4% sevoflurane [44071; Maruishi, Japan] in air in an anesthesia agent evaporator chamber for 5 h) or to the control group (exposed to air for 5 h; n = 6 per group). The body weights of the mice were assessed 6 days postnatal and 8 weeks after air or sevoflurane treatment.

Arterial blood gas and arterial blood pressure analysis

To perform arterial blood-gas analysis, arterial blood samples (100 μL) were extracted from the left cardiac ventricle of the mice before and after treatment with sevoflurane or air with a 24-gauge catheter. Arterial $PaCO_2$, PH, SaO_2, and PaO_2 were assessed with a Nova Biomedical blood gas apparatus (ABL800; Radiometer, Copenhagen, Denmark). Moreover, BIOPAC MP150 and AcqKnowledge software (Biopac Systems, Goleta, CA, USA) were used to calculate the MAP.

Primary neuronal culture

Postnatal day 1 C57BL/6 mice were used for cell culture preparation based on a protocol modified from Malgaroli and Tsien.[21] Cerebral hippocampi were separated and dissected in HEPES-buffered saline (HBS) after removing the meninges. Tissue fragments were then added to the separation medium (Neurobasal medium, 48 mL; 1% horse serum, 0.5 mL; 2% B27 supplement, 1 mL; and 0.25% GluMAX, 0.5 mL) and subjected to mild trypsinization in 0.25% Trypsin-EDTA at 37°C for 20 min and to repeated aspirations through a Pasteur pipette for mechanical dissociation. The cell suspension was pelleted by gentle centrifugation (2,000 rpm for 3 min at room temperature) and then seeded in the dissociation medium in 3.5 cm culture dishes with a specific gravity of 3×10^5 cells per mL. The cells were placed in an incubator with 5% CO_2 at 37°C.

Cell culture

Mouse hippocampal neuronal cell lines (HT22) were bought from Procell Life Science & Technology (Wuhan, China) and hatched in Dulbecco's modified Eagle's medium (DMEM) containing 15% fetal bovine serum (Invitrogen, Shanghai, China) in a 37°C incubator with 5% CO_2.

Anesthesia treatment

Primary hippocampal neurons and HT22 cells in culture dishes were randomly exposed to 3.4% sevoflurane in fresh gas (5% CO_2, 21% O_2, and balanced N_2) for 5 h (group S) or only to fresh gas (group C) at 37°C in a chamber (RWD Life Science, Shenzhen, China). A steady concentration of 3.4% sevoflurane was kept during the experiments by a Capnomac gas monitor (Datex-Ohmeda, Helsinki, Finland).

Intracranial injections and transfection experiments

A stereotaxic apparatus (Kopf Instruments) was used to fix the neonatal mice. We injected 10 μL of shRNA Xist or shRNA NC (Ruibo Biotechnology, Guangzhou, China) at a rate of 0.25 mL/min intracranially into the bilateral hippocampi of the mice with the following stereotaxic coordinates: lateral, ±0.7 mm; ventral, −1.3 mm; bregma, +1.9 mm.[22] The mice were exposed to sevoflurane 1 day later. Meanwhile, HT22 cells were transfected with shRNA Xist, miR-98 mimic, or miR-98 inhibitor (Biomics Biotechnologies, Nantong, China) or were induced an overexpression of EDEM1 via plasmid with Lipofectamine 2000 (Invitrogen; 11668-019) following the manufacturer's protocol. Subsequently, cells were gathered for EDEM1, CHOP, Trib3, Bcl-2, Bax, and caspase-3 assay using western blot analysis and quantitative real-time PCR after receiving either fresh air or 3.4% sevoflurane for 5 h.

Western blot

Radioimmunoprecipitation assay (RIPA) lysis buffer (Boster Biotechnology, Wuhan, China) and phenylmethanesulfonyl fluoride (Boster Biotechnology, Wuhan, China) were used to homogenize the

hippocampus or cells. The protein concentration was tested by a BCA kit (Beyotime Biotechnology, Haimen, China). Specific monoclonal antibodies anti-EDEM1 (sc-377394), anti-CHOP (sc-7351), anti-Trib3 (sc-365842; 1:1,000 dilution; Santa Cruz, USA), anti-cleaved caspase-3 (9664S), anti-Bcl-2 (3498S), anti-Bax (2772S), and anti-GAPDH (5174S; 1:1,000 dilution; Cell Signaling Technology, USA) were applied to hatched blots overnight at 4°C. Subsequently, the samples were hatched by horseradish peroxidase-labeled second antibody rabbit anti-mouse (5127) or mouse anti-rabbit antibody (93702; 1:5,000 dilution; Cell Signaling Technology, USA) for 2 h. The protein band absorbance was visualized by the Super Signal West Pico Chemiluminescent Substrates (Pierce Biotechnology, Rockford, IL, USA) and quantified by GEL-PRO ANALYZER software (Bio-Rad Laboratories, Hercules, CA, USA).

Quantitative real-time PCR

Total RNA was obtained by TRIzol Reagent RNAiso Plus (Takara Bio, Shiga, Japan). For lncRNA and mRNA, PrimeScript RT Reagent Kit with Genomic DNA (gDNA) Eraser (Perfect Real Time; RR047A; Takara Bio, Shiga, Japan) was used to inverse transcribe cDNA following the manufacturer's instructions. For miRNA, the reverse transcription was performed with Mir-X miRNA First-Strand Synthesis Kit (638313; Takara Bio, Shiga, Japan). Quantitative real-time PCRs were conducted in the Step One Plus Real-Time PCR System (Thermo Fisher Scientific, Waltham, MA, USA) and analyzed with TB Green Premix Ex Taq (RR420A; Takara Bio, Shiga, Japan). The reaction conditions were as follows: 95°C for 10 s, 40 cycles of 5 s at 95°C, and 30 s at 60°C. The relative gene-expression levels were detected based on the $2^{-\Delta\Delta Ct}$ method. The primer sequence of quantitative real-time PCR is shown in Table S2. β-actin and U6 were used as the internal control for Xist and miR-98-5p, respectively.

TUNEL analysis

5% formaldehyde in 0.1 M phosphate-buffered saline (PBS; Gibco; 18912-014) was used to fix the brains of the mice for 24 h at 4°C. Afterward, TUNEL staining was performed using a cell death detection kit (Roche Diagnostics, Mannheim, Germany) following the manufacturer's protocol after preparation of paraffin-embedded sections (5 μm). The apoptotic cell nuclei turned brown in diaminobenzidine chromogenic liquid (K5007; Dako, Denmark). Images were obtained with a DFC295 digital camera and edited with a DM2500 bright-field light microscope with Leica Application Suite 4.1.0 software at 200× magnification and with Adobe Photoshop CS5 version 12.1.32. The number of TUNEL-positive cells and the total number of cells in each view were determined by Image-Pro Plus software, and the apoptotic index was defined as the ratio of TUNEL-positive cells to total cells in each view.

Apoptotic cell assay

Cells were stained with Annexin V-FITC and PI with an Annexin V-FITC/PI Apoptosis Detection Kit (Becton Dickinson [BD], San Jose, CA, USA) following the manufacturer's instructions after having been gathered and washed twice with cold PBS and suspended in 1× binding buffer. The apoptosis percentage was calculated through BD fluorescence-activated cell sorting Accuri C6 (BD, San Jose, CA, USA). Data were analyzed using FlowJo software (Tree Star, Ashland, OR, USA).

Immunofluorescence analysis for EDEM1 in neurons

5% formaldehyde in 0.1 M PBS (Gibco; 18912-014) was used to immobilize the HT22 cells at 4°C for 24 h. Then, the cells were washed with PBS, fixed in 4% PBS-buffered paraformaldehyde, and permeabilized by 0.2% Triton X-100. The cells were hatched in blocking solution (10% goat serum, 1% BSA/PBS) with primary antibody, rabbit anti-active EDEM1 (1:100, sc-377394) overnight at 4°C, which was followed by dyeing with Alexa Green fluorescent and 4-6-diamidino-2-phenylindole-dihydrochloride (DAPI; 1:500; Sigma; SLBR3299 V) for 2 h to visualize the nuclei. A fluorescence microscope (Leica DM1600; Leica Microsystems, Heidelberg, Germany) and a digital camera were used to visualize the cells and record representative areas.

RIP

As mentioned in a previous study,[23] the RIP assay was performed following the manufacturer's instructions of the EZ-Magna RIP Kit (Millipore, Bedford, MA, USA). The HT22 cells were transfected with miR-98-5p mimic or control for 48 h and then resuspended in RIPA buffer and incubated on ice for 30 min. Mouse anti-Ago2 antibody (Millipore) was added into the lysate obtained by centrifugation and incubated for 4 h at 4°C; normal mouse immunoglobulin G (IgG; Santa Cruz, USA) was used as NC. Beads were suspended in RIPA buffer and processed with 45 protease K for 45 min at 45°C. RIP samples were extracted by TRIzol and detected by quantitative real-time PCR analysis.

Dual-luciferase reporter gene assay

As previously reported, the binding sites between miR-98-5p and Xist or miR-98-5p and EDEM1 were predicted by TargetScan and Starbase software, and their interaction was confirmed by the luciferase reporter assay (Data S1).[6] pGL3 (3577193; Promega, Madison, WI, USA) cloned the target fragments called Xist WT and EDEM1 WT. To create the Mut vectors of lncRNA Xist Mut type and EDEM1 Mut, site-specific mutagenesis was analyzed in the binding site of miR-98-5p and lncRNA Xist. The pRL-TK vector was used as an internal control. HT22 cells were co-transfected with 500 ng pRL-TK vector, 500 ng firefly luciferase expression vector pGL3-Xist, or pGL3-EDEM1 (XIST WT, EDEM1 WT, XIST Mut, or EDEM1 Mut) and 50 nM miR-98-5p mimic or its NC by Lipofectamine 2000. The luciferase activity was assessed in the collected cells after hatching for 48 h according to the protocols of the dual-luciferase reporter gene test kit (E1910) on the GloMax 20/20 fluorescence detector (Promega, Madison, WI, USA), and it was determined as the value of firefly luciferase activity/value of Renilla luciferase activity.

Elevated plus maze

The elevated plus maze included two enclosed arms (50 cm × 10 cm × 40 cm), a junction area (10 cm × 10 cm), and two open arms (50 cm × 10 cm). First, each mouse was put in the middle area confronting one open arm and was allowed to explore the maze for 5 min.

The total distance traveled during the experiment (locomotion index), the ratio of time spent in the open arms of the maze relative to the closed arms, and the percentage of entries into the open arms divided by the total number of entries were calculated by the EthoVision video-tracking system (Noldus Information Technology, Leesburg, VA, USA) and used as an operational definition of activity-independent anxiety.

Open field test

The spontaneous motor activity and the exploratory behaviors of the mice 8 weeks after exposure to sevoflurane were evaluated by the open field test. The test was conducted according to the study of Nikiforuk et al.[24] First, the mice were gently put into the new trail surrounding for 10 min to familiarize with it before the test began. Then, the mice exercised in a round open arena (100 cm diameter, 50 cm high). The arena was divided equally into 8 parts. The center of the arena was illuminated by a bright lamp. Each mouse was placed in the center of the field and surveyed for 5 min before starting. The activities of the mouse traveling through the open field chamber for 5 min were recorded by the Any-Maze animal tracking system software (Xinruan, Shanghai, China). The total distance traveled and the time spent in the center of the field were also registered by the software.

Three-chamber social interaction

Sociability deficits were assessed by the three-chamber social approach task 8 weeks after sevoflurane exposure as previously described.[25] The instrument was a rectangular box with three chambers of 20 cm (length) × 40.5 cm (width) × 22 cm (height). A small hole of 10 cm width × 5 cm height in the dividing Plexiglas walls allowed the mice to enter every chamber. The center chamber was the starting point. A mineral water bottle on top of the chambers hindered climbing. The time spent in each chamber and the number of transitions were recorded by an automated photo beam on each doorway. First, the test mice were habituated to the box for 10 min. Then the mice were limited to the middle chamber by means of dividers, and a novel stimulus mouse and a novel object were put in either of the two side chambers (social preference). Afterward, the dividers were removed, and the test mice were permitted to run for 10 min between the chambers with the novel stimulus mouse and the novel object. Subsequently, the test mice were limited to the middle chamber once more, and the novel object was changed for a second novel stimulus mouse (social novelty). The test mice were allowed to run again from the middle chamber and to travel for 10 min between the chambers with the familiar and new stimulus mice. The EthoVision (Noldus) was used to record the behavior sessions and the time that each test mouse spent close to and/or interacting with (sniffing and nose poking) the object or stimulus mice.

Statistical analysis

All data are present as mean ± standard deviation, and SPSS 24.0 (SPSS, Chicago, IL, USA) was used for all statistical analyses. Student's t test and two-way ANOVA, followed by post hoc tests with Bonferroni correction, were used to analyze numerical data. $p < 0.05$ was considered statistically significant.

SUPPLEMENTAL INFORMATION

Supplemental information can be found online at https://doi.org/10.1016/j.omtn.2021.04.010.

ACKNOWLEDGMENTS

This work was supported by the National Natural Science Foundation of China (81400929, 81471240, 81641042, and 81603545); Exploration Project of Zhejiang Natural Science Foundation (LY21H090006); Zhejiang Health Science and Technology Planning Project (2021KY768); Bureau of Chinese Medicine, Zhejiang, China (2018ZB065); and Innovative Talents Project of Zhejiang Province (2016).

AUTHOR CONTRIBUTIONS

L.X. conceived and designed the experiments and wrote the manuscript. Q.X., S.D., C.J., and Y.T. performed the experiments. J.X. and H.W. contributed to data analysis and manuscript preparation. X.C. contributed to the conception of the study and to manuscript revision.

DECLARATION OF INTERESTS

The authors declare no competing interests.

REFERENCES

1. Song, S.Y., Meng, X.W., Xia, Z., Liu, H., Zhang, J., Chen, Q.C., Liu, H.Y., Ji, F.H., and Peng, K. (2019). Cognitive impairment and transcriptomic profile in hippocampus of young mice after multiple neonatal exposures to sevoflurane. Aging (Albany NY) *11*, 8386–8417.

2. Satomoto, M., Sun, Z., Adachi, Y.U., Kinoshita, H., and Makita, K. (2018). Sevoflurane preconditioning ameliorates lipopolysaccharide-induced cognitive impairment in mice. Exp. Anim. *67*, 193–200.

3. Yu, X., Zhang, F., and Shi, J. (2018). Neonatal exposure to sevoflurane caused cognitive deficits by dysregulating SK2 channels and GluA2-lacking AMPA receptors in juvenile rat hippocampus. Neuropharmacology *141*, 66–75.

4. Cabrera, O.H., Tesic, V., Tat, Q.L., Chastain, S., Quillinan, N., and Jevtovic-Todorovic, V. (2020). Sevoflurane-induced dysregulation of cation-chloride cotransporters NKCC1 and KCC2 in neonatal mouse brain. Mol. Neurobiol. *57*, 1–10.

5. Gu, S., Xie, R., Liu, X., Shou, J., Gu, W., and Che, X. (2017). Long coding RNA XIST contributes to neuronal apoptosis through the downregulation of AKT phosphorylation and is negatively regulated by miR-494 in rat spinal cord injury. Int. J. Mol. Sci. *18*, 732.

6. Zhao, Q., Lu, F., Su, Q., Liu, Z., Xia, X., Yan, Z., Zhou, F., and Qin, R. (2020). Knockdown of long noncoding RNA XIST mitigates the apoptosis and inflammatory injury of microglia cells after spinal cord injury through miR-27a/Smurf1 axis. Neurosci. Lett. *715*, 134649.

7. Sun, X., Li, X., Ma, S., Guo, Y., and Li, Y. (2018). MicroRNA-98-5p ameliorates oxygen-glucose deprivation/reoxygenation (OGD/R)-induced neuronal injury by inhibiting Bach1 and promoting Nrf2/ARE signaling. Biochem. Biophys. Res. Commun. *507*, 114–121.

8. Zhu, G., Tao, L., Wang, R., Xue, Y., Wang, X., Yang, S., Sun, X., Gao, G., Mao, Z., and Yang, Q. (2017). Endoplasmic reticulum stress mediates distinct impacts of sevoflurane on different subfields of immature hippocampus. J. Neurochem. *142*, 272–285.

9. Papaioannou, A., Higa, A., Jégou, G., Jouan, F., Pineau, R., Saas, L., Avril, T., Pluquet, O., and Chevet, E. (2018). Alterations of EDEM1 functions enhance ATF6 pro-survival signaling. FEBS J. *285*, 4146–4164.

10. Lin, H., Zhou, Z., Zhong, W., Huang, P., Ma, N., Zhang, Y., Zhou, C., Lai, Y., Huang, S., An, H., et al. (2017). Naringenin inhibits alcoholic injury by improving lipid metabolism and reducing apoptosis in zebrafish larvae. Oncol. Rep. *38*, 2877–2884.

11. Lin, D., Liang, Y., Zheng, D., Chen, Y., Jing, X., Lei, M., Zeng, Z., Zhou, T., Wu, X., Peng, S., et al. (2018). Novel biomolecular information in rotenone-induced cellular model of Parkinson's disease. Gene *647*, 244–260.

12. Xu, L., Shen, J., McQuillan, P.M., and Hu, Z. (2018). Anesthetic agents and neuronal autophagy. What we know and what we don't. Curr. Med. Chem. *25*, 908–916.

13. Xu, L., Hu, Y., Huang, L., Liu, Y., Wang, B., Xie, L., and Hu, Z. (2019). The association between attention deficit hyperactivity disorder and general anaesthesia - a narrative review. Anaesthesia *74*, 57–63.

14. Satomoto, M., Satoh, Y., Terui, K., Miyao, H., Takishima, K., Ito, M., and Imaki, J. (2009). Neonatal exposure to sevoflurane induces abnormal social behaviors and deficits in fear conditioning in mice. Anesthesiology *110*, 628–637.

15. Zhou, Z.B., Yang, X.Y., Yuan, B.L., Niu, L.J., Zhou, X., Huang, W.Q., Feng, X., and Zhou, L.H. (2015). Sevoflurane-induced down-regulation of hippocampal oxytocin and arginine vasopressin impairs juvenile social behavioral abilities. J. Mol. Neurosci. *56*, 70–77.

16. Lin, D., Liu, J., Kramberg, L., Ruggiero, A., Cottrell, J., and Kass, I.S. (2016). Early-life single-episode sevoflurane exposure impairs social behavior and cognition later in life. Brain Behav. *6*, e00514.

17. Diana, P., Joksimovic, S.M., Faisant, A., and Jevtovic-Todorovic, V. (2020). Early exposure to general anesthesia impairs social and emotional development in rats. Mol. Neurobiol. *57*, 41–50.

18. Yue, D., Guanqun, G., Jingxin, L., Sen, S., Shuang, L., Yan, S., Minxue, Z., Ping, Y., Chong, L., Zhuobo, Z., and Yafen, W. (2020). Silencing of long noncoding RNA XIST attenuated Alzheimer's disease-related BACE1 alteration through miR-124. Cell Biol. Int. *44*, 630–636.

19. Yang, W., Tiffany-Castiglioni, E., Koh, H.C., and Son, I.H. (2009). Paraquat activates the IRE1/ASK1/JNK cascade associated with apoptosis in human neuroblastoma SH-SY5Y cells. Toxicol. Lett. *191*, 203–210.

20. The Ministry of Science and Technology of the People's Republic of China (2006). Guidance Suggestions for the Care and Use of Laboratory Animals.

21. Malgaroli, A., and Tsien, R.W. (1992). Glutamate-induced long-term potentiation of the frequency of miniature synaptic currents in cultured hippocampal neurons. Nature *357*, 134–139.

22. Depino, A.M., Lucchina, L., and Pitossi, F. (2011). Early and adult hippocampal TGF-β1 overexpression have opposite effects on behavior. Brain Behav. Immun. *25*, 1582–1591.

23. Tsai, M.C., Manor, O., Wan, Y., Mosammaparast, N., Wang, J.K., Lan, F., Shi, Y., Segal, E., and Chang, H.Y. (2010). Long noncoding RNA as modular scaffold of histone modification complexes. Science *329*, 689–693.

24. Nikiforuk, A., Kos, T., Fijał, K., Hołuj, M., Rafa, D., and Popik, P. (2013). Effects of the selective 5-HT7 receptor antagonist SB-269970 and amisulpride on ketamine-induced schizophrenialike deficits in rats. PLoS One *8*, e66695.

25. Yang, M., Silverman, J.L., and Crawley, J.N. (2011). Automated three chambered social approach task for mice. Curr. Protoc. Neurosci., Chapter 8:Unit 8.26.